International Journal of Mass Spectrometry 284 (2009) 152–161

Contents lists available at ScienceDirect

International Journal of Mass Spectrometry

journal homepage: www.elsevier.com/locate/ijms

# LA-ICP-MS analysis of African glass beads: Laboratory inter-comparison with an emphasis on the impact of corrosion on data interpretation

Laure Dussubieux[a,*], Peter Robertshaw[b], Micheal D. Glascock[c]

[a] Department of Anthropology, The Field Museum, 1400 South Lake Shore Drive, Chicago, IL 60605, USA
[b] Department of Anthropology, California State University, San Bernardino, CA 92407, USA
[c] Research Reactor Center, University of Missouri Columbia, Columbia, MO 65211, USA

ARTICLE INFO

*Article history:*
Received 1 February 2008
Received in revised form
24 September 2008
Accepted 12 November 2008
Available online 21 November 2008

*Keywords:*
LA-ICP-MS
Glass
Bead
Corrosion
Africa

ABSTRACT

A comparison between the compositions determined by laser ablation-inductively coupled plasma-mass spectrometry (LA-ICP-MS) from two different laboratories on 52 ancient beads recovered in Africa was undertaken. Single point and raster samplings by the laser ablation systems were used. Although similar results were obtained using the two approaches on most of the beads, raster sampling was found more sensitive to corrosion than single point sampling. The impact of corrosion on the results and on their interpretation is discussed. Depending on the types of glass, group attribution is variably affected.

## 1. Introduction

Laser ablation-inductively coupled plasma-mass spectrometry (LA-ICP-MS) is an analytical technique developed in the mid-1980s that is able to determine the elemental composition of inorganic solid samples. The advantages of this technique include low limits of detection (in the range of the part per million (ppm) or below depending on the element), rapidity of analysis (a few minutes per sample), high spatial resolution and minimum damage to the sample. It has been used in a number of different fields including geology, material science, biology, medicine and archaeology beginning in the 1990s [1,2]. Glass is one of the most studied materials using this technique, more especially for forensic applications (see for example [3–5]) but also to address archaeological questions [6]. The accurate determination of ancient artifact compositions by LA-ICP-MS requires that the materials under investigation are reasonably homogeneous. In previous studies on ancient glass, although the volume of matter sampled by the laser ablation system is extremely small, it has been found to be representative of the whole object [6,7]. Moreover, the availability of matched-matrix standard reference materials allows the reliable determination of 50–60 major, minor and trace elements [8].

The low detection limits offered by LA-ICP-MS have created new avenues of research based on the study of trace element patterns in glass, including better definition and more reliable differentiation of existing glass types, as well as studies of provenance. In the pioneering work of Saitowitz [9] and Saitowitz et al. [10], LA-ICP-MS was used to determine the trace element concentrations for several African, South and Southeast Asia glass beads in tandem with scanning electron microscopy-energy dispersive X-ray spectrometry measurements for the major and minor elements. Provenance attributions for the African beads were made by matching rare earth elements (REE) patterns, notably cerium and europium anomalies, in the African beads with samples from different glass producing areas; however, Saitowitz's results were unconvincing because she found similar trace element patterns for different glass compositions unlikely to have been made in the same area. A decade later, Robertshaw et al. [11], using LA-ICP-MS to determine the major, minor and trace elements in glass beads according to the method developed in the meantime by Gratuze [8], compared the rare earth anomalies in glass samples found in Madagascar, dated from 9th to 15th c. A.D. to different types of rocks. Similarities with basalt and granite rocks abundant in the South and Southeast Asian region were found which supported provenance assignments for the glass beads to these regions.

In general, the usefulness of the LA-ICP-MS technique for the routine determination of a large number of trace elements in order to characterize ancient glass has been demonstrated in a number of research projects. De Raedt et al. [12] and Šmit et al. [13]

---

[*] Corresponding author.
*E-mail address:* ldussubieux@fieldmuseum.org (L. Dussubieux).

1387-3806/$ – see front matter © 2008 Elsevier B.V. All rights reserved.
doi:10.1016/j.ijms.2008.11.003

characterized Venetian and façon-de-Venise glass vessels of the 16th and 17th c. A.D. from, respectively, Antwerp (Belgium) and Slovenia. It has also been shown to be possible to discriminate a local soda-lime glass found at early South and Southeast Asia sites from soda-lime glass samples imported from the Syro-Palestinian region as the former has slightly higher trace element concentrations than the latter [14]. Furthermore, different trace element patterns were identified for Mesopotamian and Egyptian Bronze Age glass samples enabling provenance attribution [15]. Finally, two different types of alumina glasses, abundant in Africa and India and exhibiting correlations between geographical areas, time periods and trace element patterns have been identified [16].

The sensitivity of LA-ICP-MS for a large range of elements is one of the major advantages of this analytical technique. Moreover, its quasi-non-destructiveness and the rapidity of the analysis, which allow for the investigation of large sets of representative samples, are also largely responsible for significant advances in the field of ancient glass studies over the past 10 years. In one such recent study, Robertshaw performed analysis of about 1000 glass beads from Africa with LA-ICP-MS. Archaeological samples from the southern African interior, Zambia, the East African coast, Uganda, West Africa, and Morocco were investigated to identify the regions where the glass was manufactured and to reconstruct changing patterns of trade through time within Africa and between this continent and other regions of the world. Eventually conclusions derived from this study of glass beads will be compared to what is known about other types of artifacts to investigate whether different types of material culture that were imported to Africa came from the same or different regions. Most of the glass beads were analyzed at the Archaeometry Laboratory at the University of Missouri Research Reactor (MURR). The instrumentation and the analytical protocol are described in Popelka et al. [17] along with some preliminary results. More analytical results are available in Robertshaw et al. [11,18]. A total of 166 glass bead samples were analyzed in the LA-ICP-MS laboratory at the field museum (FM) and among these were 52 that were analyzed by both laboratories, allowing the inter-comparability of the data produced by the two laboratories to be assessed.

In this article, the analytical results for these 52 samples are presented and two issues related to LA-ICP-MS analysis of ancient glass are examined. After a description of the instrumentation, analytical protocol and performances of the LA-ICP-MS at the field museum for glass analysis, the degree of comparability between the results produced by the MURR and the FM laboratories is assessed. This part of the study was found necessary due to the increasing number of LA-ICP-MS data produced by different laboratories and subsequent questions about their inter-comparability. Since, generally, no sample preparation is necessary when using LA-ICP-MS, in the case of corroded samples, the results can be different. The impact of corrosion on glass composition and how this affects group attribution of samples and therefore data interpretation is also evaluated.

## 2. Experimental

### 2.1. Instrumentation and analytical parameters at the MURR archaeometry lab

The instrumentation at MURR comprises a VG axiom double-focusing high-resolution ICP-MS connected to a Merchantek 213 nm Nd:YAG laser ablation system. Sampling of the artifacts were conducted with the laser ablation system operating at 50% of its full energy (i.e., 0.4 mJ), using the scan mode with a laser beam diameter of 100 μm, a speed of 70 μm/min and a frequency of 20 Hz. Two pre-ablation passes were performed prior to data acquisition to remove possible surface contamination and corrosion.

To obtain quantitative results, internal and external standardizations were used. The $^{30}$Si isotope was selected as an internal standard. External standards include National Institute of Standards and Technology (NIST) standard reference materials (SRM) 610 and 612, Corning glasses B, C and D and obsidian from Glass Buttes, Oregon and Sierra de Pachuca, Mexico. Concentrations were calculated according to Gratuze et al. [7], Neff [19] and Speakman and Neff [20]. More details on the analytical method at MURR and its performance can be found in Popelka et al. [17].

### 2.2. Instrumentation and analytical parameters at the Field Museum

The analyses carried out at FM involved a Varian ICP-MS and a New Wave UP213 laser, for direct introduction of solid samples. The parameters for ICP-MS were optimized to ensure a stable signal with a maximum intensity over the full range of masses of the elements and to minimize oxides and double ionized species formation ($CeO^+/Ce^+$ and $Ba^{2+}/Ba^+ < 1–2\%$). For that purpose the argon flows, the radio-frequency power, the torch position, the lenses, the mirror and the detector voltages were adjusted using an auto-optimization procedure. For better sensitivity, helium is used as a gas carrier in the laser. To be able to determine elements with concentrations in the range of ppm and below while leaving a trace on the surface of the sample invisible to the naked eye, the single point analysis mode with a laser beam diameter of 55 μm, operating at 70% of the laser energy (0.2 mJ) and at a pulse frequency of 15 Hz was used. A pre-ablation time of 20 s was set up in order, first, to eliminate the transient part of the signal and, second, to be sure that a possible surface contamination or corrosion does not affect the results of the analysis. For each glass sample, an average of four measurements corrected from the blank is considered for the calculation of concentrations.

Silica is the most abundant component in most ancient glasses and therefore $^{29}$Si isotope was used for internal standardization. Isotope $^{29}$Si is often preferred to isotope $^{30}$Si as the $NO^+$ species is producing a high background at mass ($m/z$) 30. Concentrations for major components, including silica, were calculated assuming that the sum of their concentrations in weight percent of oxide in glass is equal to 100% [8].

Two different series of standard reference materials were used to determine the concentrations of major, minor and trace elements. The first series of external standards were NIST SRM 610 and 612. Both these standards are soda-lime-silica glass doped with trace elements in the range of 500 ppm (SRM 610) and 50 ppm (SRM 612). Certified values are available for a very limited number of elements. Concentrations from Pearce et al. [21] were used for the other elements. The second series of standards were manufactured by Corning. Glasses B and D best match the compositions of ancient glass [22]. Glass Corning C is generally not one of the standards used for quantitative analysis but is measured regularly to check the reliability of our results.

### 2.3. Evaluation of the LA-ICP-MS protocol to determine the composition of ancient glass at the field museum

To evaluate the performance of the FM method, the detection limits, reproducibility and accuracy of the protocol were determined.

The detection limits were calculated as three times the standard deviation obtained from the measurement of 10 blanks. Ideally, these detection limits would have been determined from multiple measurements on a pure silica material to take into account the contribution of the silica matrix to the background, but such a material was not available. Therefore the limits of detection may

**Table 1**
Comparison between the composition of Corning Glass B measured by LA-ICP-MS at the field museum (FM), with accuracy and reproducibility, with the composition published by Brill [22]. The composition measured by MURR [17] and the relative deviation between the FM and MURR results are also reported. In this table, n.r. is not reported.

| | Brill (1999) | FM | Accuracy | Reproducibility | MURR | Relative deviation between the FM and MURR results |
|---|---|---|---|---|---|---|
| $SiO_2$ | n.r. | 61.5% | n.r. | 1% | 63.8 ± 0.7% | 4% |
| $Na_2O$ | 17.0% | 17.6% | 4% | 2% | 15.4 ± 1.2% | 13% |
| MgO | 1.03% | 1.01% | 2% | 4% | 1.04 ± 0.08% | 3% |
| $Al_2O_3$ | 4.36% | 4.38% | 0% | 2% | 4.74 ± 0.26% | 8% |
| $P_2O_3$ | 0.82% | 0.81% | 1% | 3% | 0.60 ± 0.21% | 26% |
| $K_2O$ | 1.00% | 1.06% | 6% | 6% | 1.03 ± 0.12% | 3% |
| CaO | 8.56% | 8.95% | 5% | 2% | 9.13 ± 0.27% | 2% |
| $Sb_2O_5$ | 0.46% | 0.46% | 0% | 2% | 0.45 ± 0.07% | 2% |
| MnO | 0.25% | 0.25% | 1% | 2% | 0.22 ± 0.01% | 12% |
| $Fe_2O_3$ | 0.34% | 0.37% | 8% | 28% | 0.27 ± 0.01% | 27% |
| CuO | 2.66% | 2.63% | 1% | 4% | 2.31 ± 0.17% | 12% |
| $SnO_2$ | 0.040% | 0.029% | 28% | 6% | 0.021 ± 0.001% | 28% |
| $PbO_2$ | 0.61% | 0.53% | 13% | 25% | 0.45 ± 0.04% | 15% |
| BaO | 0.12% | 0.07% | 38% | 4% | 0.08 ± 0.02% | 14% |
| ZnO | 0.19% | 0.20% | 5% | 4% | 0.17 ± 0.03% | 15% |
| $TiO_2$ | 0.09% | 0.10% | 7% | 12% | 0.10 ± 0.02% | 0% |
| $V_2O_3$ | 0.04% | 0.03% | 7% | 5% | 0.031 ± 0.002% | 3% |
| NiO | 0.10% | 0.09% | 8% | 4% | 0.082 ± 0.008% | 9% |
| SrO | 0.019% | 0.019% | 1% | 13% | 0.0167 ± 0.0003% | 12% |

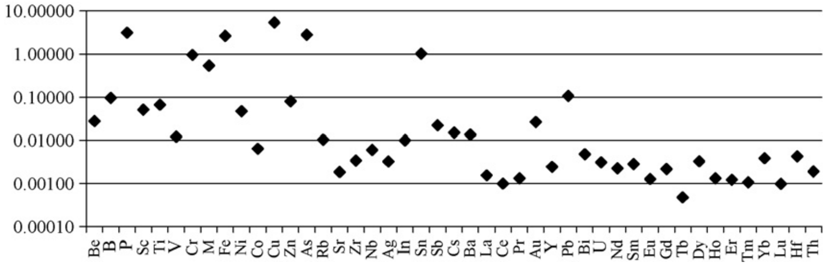

**Fig. 1.** Limits of detection in ppm for the FM LA-ICP-MS protocol.

have been slightly underestimated. Using the analytical protocol defined above, the detection limits range from less than 1 ppb to 2 ppm for copper and are generally under 1 ppm for most of the elements (Fig. 1). As the instrument is also used for copper analysis, it is likely that the high detection limit for this element is due to some contamination of the instrument.

Accuracy for the elements of interest in this study was assessed by analyzing three standard reference materials, Corning glasses B, D and C, under the same conditions as the glass bead samples. Accuracy is the relative deviation between the published concentrations and the average concentrations measured by LA-ICP-MS at FM for the standard reference materials.

For the Corning glasses B and D, the reproducibility of results was calculated as the relative standard deviation (R.S.D.) on the 20 measurements performed on the same reference materials over a period of approximately 2 years. Only five measurements were taken into account for Corning glass C.

Tables 1–3 report the accuracy and reproducibility of the FM measurements for those elements for which concentrations are available in Brill [22]. Average concentrations with their standard

**Table 2**
Comparison between the composition of Corning Glass D measured by LA-ICP-MS at the field museum (FM), with accuracy and reproducibility, with the composition published by Brill [22]. The composition measured by MURR [17] and the relative deviation between the FM and MURR results are also reported. In this table, n.r. is not reported.

| | Brill (1999) | FM | Accuracy | Reproducibility | MURR | Relative deviation between the FM and MURR results |
|---|---|---|---|---|---|---|
| $SiO_2$ | n.r. | 55.6% | n.r. | 1% | 56.5 ± 1.0% | 2% |
| $Na_2O$ | 1.20% | 1.46% | 22% | 10% | 1.65 ± 0.35% | 13% |
| MgO | 3.94% | 3.95% | 0% | 2% | 3.76 ± 0.31% | 5% |
| $Al_2O_3$ | 5.30% | 5.36% | 1% | 2% | 5.96 ± 0.14% | 11% |
| $P_2O_3$ | 3.93% | 3.94% | 0% | 4% | 3.07 ± 0.85% | 22% |
| $K_2O$ | 11.3% | 11.4% | 1% | 1% | 9.39 ± 0.56% | 18% |
| CaO | 14.8% | 15.0% | 1% | 3% | 16.0 ± 1.4% | 7% |
| $Sb_2O_5$ | 0.97% | 0.97% | 0% | 2% | 0.96 ± 0.09% | 1% |
| MnO | 0.55% | 0.56% | 2% | 3% | 0.557 ± 0.007% | 1% |
| $Fe_2O_3$ | 0.52% | 0.53% | 1% | 26% | 0.41 ± 0.01% | 23% |
| CuO | 0.38% | 0.37% | 1% | 5% | 0.37 ± 0.07% | 0% |
| $SnO_2$ | 0.10% | 0.10% | 2% | 6% | 0.08 ± 0.01% | 20% |
| PbO | 0.48% | 0.28% | 43% | 12% | 0.23 ± 0.01% | 18% |
| BaO | 0.51% | 0.27% | 46% | 8% | 0.38 ± 0.09% | 40% |
| ZnO | 0.10% | 0.10% | 0% | 3% | 0.090 ± 0.007% | 10% |
| $TiO_2$ | 0.38% | 0.34% | 12% | 6% | 0.39 ± 0.11% | 15% |
| $V_2O_3$ | n.r | 0.017% | n.r | 6% | 0.017 ± 0.001% | 0% |
| NiO | n.r. | 0.047% | n.r | 4% | 0.046 ± 0.05% | 2% |
| SrO | 0.057% | 0.058% | 1% | 5% | 0.065 ± 0.001% | 12% |

**Table 3**
Comparison between the composition of Corning Glass C measured by LA-ICP-MS at the field museum (FM), with accuracy and reproducibility, with the composition published by Brill [22]. The composition measured by MURR [17] and the relative deviation between the FM and MURR results are also reported. In this table, n.r. is not reported.

| | Brill (1999) | FM | Accuracy | Reproducibility | MURR | Relative deviation between the FM and MURR results |
|---|---|---|---|---|---|---|
| $SiO_2$ | n.r. | 33.6% | n.r | 3% | 35.6 ± 0.5% | 6% |
| $Na_2O$ | 1.07% | 1.07% | 0.4% | 7% | 1.10 ± 0.06% | 3% |
| MgO | 2.76% | 2.58% | 7% | 5% | 2.39 ± 0.14% | 7% |
| $Al_2O_3$ | 0.87% | 0.83% | 5% | 6% | 1.01 ± 0.04% | 22% |
| $P_2O_3$ | 0.14% | 0.06% | 55% | 7% | 0.07 ± 0.03% | 17% |
| $K_2O$ | 2.84% | 2.92% | 3% | 4% | 2.54 ± 0.13% | 13% |
| CaO | 5.07% | 5.84% | 15% | 10% | 5.74 ± 0.22% | 2% |
| $Sb_2O_5$ | 300 | 0.00014% | 100% | 9% | 0.00020 ± 0.00005% | 43% |
| MnO | n.r. | 0.0015% | n/a | 13% | 0.0013 ± 0.0002% | 13% |
| $Fe_2O_3$ | 0.34% | 0.31% | 10% | 6% | 0.24 ± 0.03% | 23% |
| CuO | 1.13% | 1.17% | 4% | 6% | 1.07 ± 0.05% | 9% |
| $SnO_2$ | 0.19% | 0.19% | 2% | 3% | 0.17 ± 0.02% | 11% |
| PbO | 36.7% | 40.2% | 10% | 2% | 36.2 ± 2.0% | 10% |
| BaO | 11.4% | 11.1% | 3% | 4% | 12.5 ± 1.5% | 13% |
| ZnO | 0.052% | 0.052% | 2% | 2% | 0.043 ± 0.006% | 17% |
| $TiO_2$ | 0.79% | 0.72% | 9% | 1% | 0.73 ± 0.18% | 1% |
| $V_2O_3$ | n.r. | 0.0074% | n.r | 5% | 0.0063 ± 0.0005% | 15% |
| NiO | n.r. | 0.020% | n.r | 6% | 0.018 ± 0.003% | 10% |
| SrO | 0.29% | 0.32% | 9% | 4% | 0.32 ± 0.04% | 0% |

deviation obtained at MURR from the multiple measurements of the Corning glasses (generally, 5–6 measurements were carried out each day) conducted on successive days are also reported in Tables 1–3. For the FM data, accuracy is generally better than 10%. For a few elements, the concentrations provided by Brill [22] and the FM values do not coincide. Comparison with concentrations obtained by Popelka et al. [17] shows a much better agreement, suggesting that the values published by Brill may have not been the best ones in a few cases.

Reproducibility is better than 10% for most elements but iron and lead have a relatively poor reproducibility. For iron, this may be linked to the use of an isotope, $^{57}$Fe, with an abundance of only 2.2%. This isotope was selected because of the interference between $^{56}Fe^+$ and $^{56}ArO^+$. For lead, the problem of reproducibility of the results is likely due to some slight contamination that occurs when a series of heavily leaded glass samples are measured causing some background intensity fluctuations at the mass of lead.

Agreement between the MURR and the FM results varies and depend on the element. The relative deviations between the FM and MURR results range from 0 to 43%. Some systematic over or underestimation for a given element may indicate a calibration problem. For example, iron and tin are always underestimated by MURR. Moreover, the selection of two different ablation modes, single spot or scan mode, has an influence on the accuracy and precision on the measurements [23] and may explain the discrepancy between the two sets of results.

## 3. Description of the samples

The 52 samples analyzed by both laboratories represent a stratified random sample, the strata being based on the dates of the original analyses at MURR. All samples but one originate from Africa (Table 4). The samples are beads or bead fragments. Some of them are visibly heavily corroded. Four additional samples were used to test the homogeneity of the archaeological samples. These samples were selected based on two criteria: they presented no visible trace of corrosion and their compositions were similar to those of the 52 samples that are part of this study. AFR2 and 3 have identical compositions. AFR1, AFR2 and AFR3 are from Africa and sample RR7 comes from Sri Lanka. The AFR samples are beads with a maximum dimension of 5–7 mm while RR7 is a raw piece of glass with a maximum dimension of 15 mm. AFR1 is opaque red, AFR2 is translucent

**Table 4**
List of the archaeological glass beads.

| Country | Site | Period | Sample references |
|---|---|---|---|
| Botswana | Bosutswe | Khami | PR115 |
| Botswana | Bosutswe | Mapungubwe | PR146 |
| Botswana | Bosutswe | Zhizo | PR153 |
| Botswana | Kgaswe | Mapungubwe | PR796 |
| Botswana | Nqoma | EIA | PR156 |
| Botswana | Nqoma | Zhizo | PR781, PR784 |
| Botswana | Tora Nju | Zimbabwe | PR158 |
| Kenya | Mwana | 2nd millennium A.D. | PR365, PR372, PR380, PR386, PR391 |
| Kenya | Shanga | 2nd millennium A.D. | PR718, PR719, PR725, PR726, PR734 |
| Kenya | Shanga | 2nd millennium A.D. | PR746, PR748, PR749, PR754, PR768 |
| Pemba (Tanzania) | Chwaka | 2nd millennium A.D. | PR471, PR475, PR479, PR480, PR481, PR483 |
| South Africa | K2 | K2 | PR020, PR064 |
| South Africa | Mapungubwe | Mapungubwe | PR080, PR090, PR793 |
| South Africa | Faure | Khami | PR105 |
| South Africa | Pont Drift | Zhizo | PR185 |
| South Africa | Schroda | Zhizo | PR212 |
| South Africa | Schroda | K2 | PR218 |
| South Africa | Skutwater | K2 | PR238 |
| South Africa | Skutwater | K2? | PR246 |
| South Africa | Thulameli | Khami | PR266, PR275, PR276, PR283 |
| Sri Lanka | Unknown | Unknown | PR205 |
| Zimbabwe | Great Zimbabwe | Zimbabwe | PR779 |

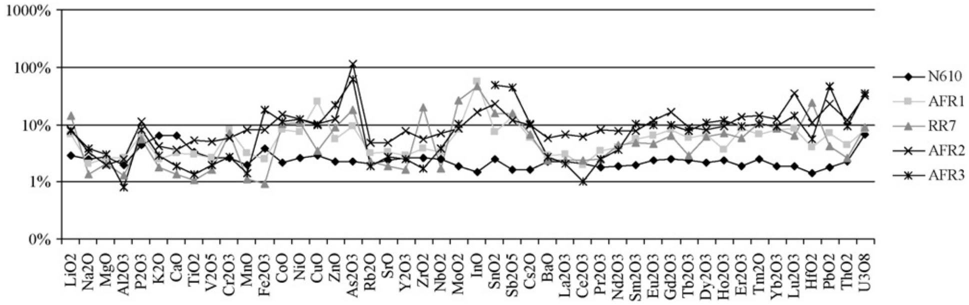

**Fig. 2.** Relative standard deviation on the 10 successive measurements performed on SRM 610 and four archaeological samples. The curves linking the symbols have no meaning; they are simply intended to offer a better visualization of the sets of results.

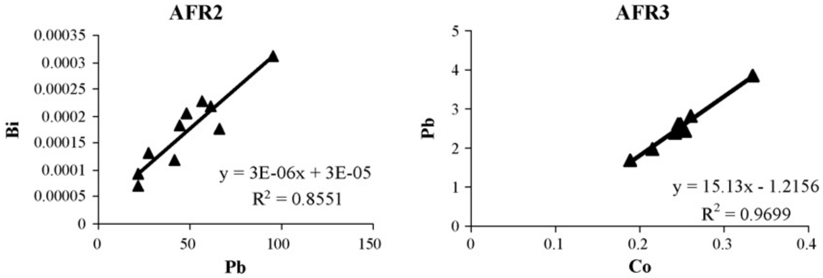

**Fig. 3.** (a and b) Normalized signal intensities of lead and bismuth in AFR2 and cobalt and lead in AFR3.

cobalt blue and AFR3 is opaque yellow. RR7 is opaque red with black veins.

## 4. Results

### 4.1. Homogeneity of ancient glass found in Africa and Sri Lanka

Before comparing the results from the MURR and FM laboratories, it is necessary to assess the impact of the heterogeneity of the glass beads on the results.

The repeatability (or precision) of results is a reflection of the homogeneity of the sample and of the stability of the instrument. Precision was calculated as the R.S.D. on the 10 successive measurements performed on a sample or SRM. For a SRM, which is assumed to be "ideally" homogeneous, the repeatability will only reflect the stability of the instrument. An archaeological sample is considered homogenous when the R.S.D. for a given element is close to the R.S.D. for the same element as calculated for the SRM (Fig. 2). To assess homogeneity, the SRM chosen was the NIST glass 610 (N610 in Fig. 2) and the four archaeological samples described in Section 3 were analyzed.

One factor, which affects the repeatability of a measurement, is the concentration of each element. Generally, the R.S.D. is low for the major elements and minor elements but sometimes higher for elements present in low concentrations (e.g., REE) particularly when the detection limits are approached. For the SRM, the repeatability is generally 5% or lower but for the archaeological samples, it is less than 20% for most of the elements. Based on the samples examined, it does not appear that some types of glass are more homogenous than others; however, a larger sample would be necessary to confirm this observation.

Elements used as coloring or opacifying agents generally show higher R.S.D. as they are dispersed in the matrix with a variable degree of homogeneity. Sample AFR2 is a cobalt blue glass with an R.S.D. for cobalt, the coloring element, of 15%. The results for magnesium, iron, nickel, copper, zinc, lead, tin and antimony show a similar dispersion. The normalized signal intensities of these elements exhibit a strong correlation with the normalized signal intensity of cobalt, with correlation coefficients ranging from 0.84 to 0.97 (Table 5 and Fig. 3a). This correlation implies that the cobalt-containing ingredient added to the glass contained all these elements, which in turn explains why we observe the same dispersion for cobalt and these other elements.

**Table 5**
Correlation coefficients for the normalized signal intensities for a range of elements with that of cobalt in sample AFR2.

| | |
|---|---|
| Mn | 0.88 |
| Fe | 0.96 |
| Ni | 0.95 |
| Cu | 0.90 |
| Zn | 0.84 |
| Pb | 0.97 |
| Sn | 0.96 |
| Sb | 0.93 |

AFR3 is an opaque yellow glass containing lead and tin. Combined as $PbSnO_3$ [24], these elements form a yellow opacifier. Lead ore can also contain elements such as arsenic, bismuth, silver and antimony. The R.S.D. calculated for this sample from lead, arsenic, tin, antimony and bismuth signal intensities are 40% and higher. Further, the correlation coefficients for lead and arsenic, tin, antimony and bismuth are higher than 0.85 indicating that all of these elements were added to the glass batch as a unique ingredient (Table 6 and Fig. 3b).

As shown for samples AFR2 and 3, LA-ICP-MS is a powerful tool for determining which elements, even at the trace level, are associated with each other. From these results, it seems reasonable to conclude that the homogeneity of ancient glass is such that the variability in signal intensities is less than 20% for most of the ele-

**Table 6**
Correlation coefficients for the normalized signal intensities for a range of elements with that of lead in sample AFR3.

| | |
|---|---|
| As | 0.86 |
| Sn | 0.88 |
| Sb | 0.87 |
| Bi | 0.86 |

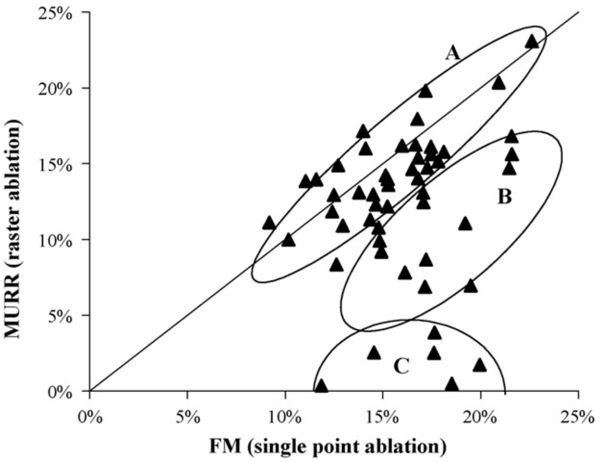

**Fig. 4.** Plot of the soda concentration measured by FM and MURR for each of the 52 archaeological glass bead samples.

ments not involved in the coloring or opacifying process of the glass. Exceptions have to be considered on a case-by-case basis depending on the colorant used.

### 4.2. Archaeological glass bead samples: comparison of the results when there is no corrosion

The 52 archaeological glass bead samples are all silica glasses with soda as the second most abundant constituent. In order to compare the results from the MURR and FM laboratories, first those samples for which compositions, as measured by the FM laboratory, appeared unaffected by corrosion, were selected. Comparison of the results produced by both laboratories shows that some of the MURR compositions are strongly depleted in soda, which is a sign that corroded glass was sampled. The use of the raster mode for ablation at MURR compared to the point mode with a pre-ablation time of approximately 20 s used by the FM laboratory implies that the analyzed glass was sampled less deeply under the surface at MURR and so had more chance to be affected by corrosion. Fig. 4 reports the soda concentrations for the FM and MURR laboratories. When the FM and MURR measurements are very similar, the data points fall close to the $y = x$ curve in Fig. 4. The samples in Group A have similarly high soda concentrations as recorded by both laboratories and were probably the least affected by corrosion. In Group C, six samples are highly soda-depleted according to MURR measurements. These glass samples will be discussed later in Section 4.3 and represent highly corroded glass. Samples with a MURR composition variably affected by corrosion fall in Group B.

From within Group A, the samples with the smallest relative deviations calculated from the two series of soda concentrations derived from the MURR and FM measurements were selected. Twelve samples (PR080, PR105, PR115, PR156, PR158, PR185, PR205, PR910, PR921, PR481, PR483, and PR725) have deviations for soda concentrations ranging from 1% to a maximum of 8%. Therefore, for these 12 samples, it can be assumed that the differences in composition observed between the two laboratories are not due to corrosion.

Fig. 5 shows the minimum, maximum and average relative deviations between the MURR and FM laboratories for all the elements in these 12 non-corroded glass samples. For most elements, the average deviation is approximately 20%, which can be explained by the heterogeneity of the glass and also by the fact that different instrumentations and protocols were employed. However, significantly higher deviations were observed for several elements: phosphorus, iron, arsenic, indium, tin, antimony and lead.

For most samples, the discrepancy between the indium concentrations measured by MURR and FM is rather large. The most abundant isotope for indium is at mass 115, which is also the mass for one of the isotopes of tin. A correction is undertaken to subtract the contribution of $^{115}$Sn at the mass 115; however, as indium is always a trace element whereas tin can be in the glass with relatively high concentrations, use of this correction can lead to considerable imprecision for the signal intensity for indium. Indium is was found important in only one case: this element is associated with cobalt in certain ores and thus can be used to help pin point the provenance of the cobalt ore added as a colorant in cobalt blue glass [25,26].

Iron measurement presents problems because of the selection of an isotope with a low abundance to avoid major interference (as discussed in Section 2.3). For phosphorus, the ionization of this element is difficult in an argon plasma because this element has a relatively high ionization energy (10.486 eV). Besides, the determination of phosphorus is disturbed by the interfering species $^{14}N^{16}OH^+$ and the adjacent large peak produced by $^{16}O_2{}^+$ due to contamination from ambient air. The other elements, arsenic, tin, antimony and lead are often associated with coloring ingredients and may be heterogeneously distributed in the glass. However, in summary, when glass samples are not corroded, the results from the MURR and the FM laboratories agree quite well, with the exception of a few elements.

### 4.3. Archaeological glass bead samples: comparison of the results for the highly corroded glass

Glass corrosion is a result of the interaction of the glass surface with water. It is a complex process including dissolutions and pre-

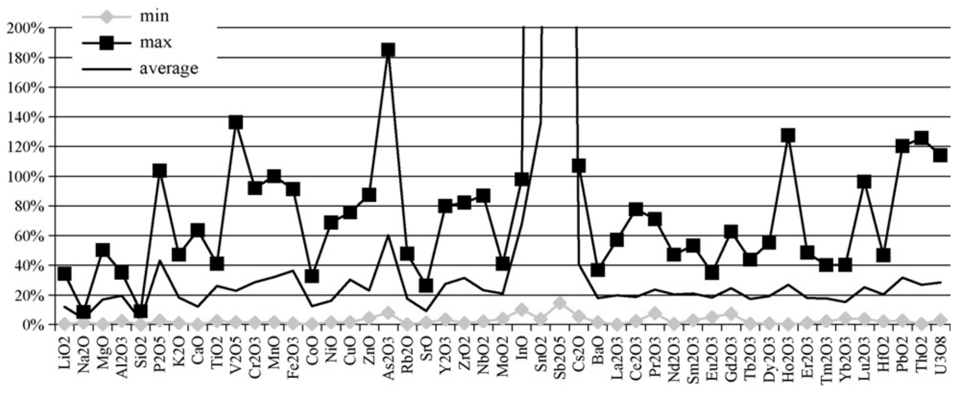

**Fig. 5.** Minimum, maximum and average relative deviations between the MURR and FM concentrations measured for each element for the 12 non-corroded glass bead samples. The curves linking the symbols have no meaning; they are simply intended to offer a better visualization of the sets of results.

**Table 7**
Percentages of depletion or enrichment for the glass-forming elements (italics) and the network-modifying elements in corroded part of the samples compared to the pristine composition of the glass.

| | PR781 | PR793 | PR768 | PR796 | PR719 | PR746 |
|---|---|---|---|---|---|---|
| *Si* | *−3%* | *24%* | *19%* | *15%* | *13%* | *5%* |
| Na | −97% | −97% | −91% | −86% | −82% | −78% |
| Mg | −78% | −78% | 20% | −90% | −70% | 68% |
| K | −77% | −31% | 51% | −53% | −58% | 59% |
| Ca | −13% | −17% | 12% | 4% | −23% | 30% |
| *Al* | *173%* | *125%* | *40%* | *129%* | *315%* | *73%* |
| *Fe* | *371%* | *162%* | *33%* | *184%* | *−59%* | *−8%* |
| *Ti* | *628%* | *195%* | *28%* | *378%* | *14%* | *108%* |

cipitations of the ionic species in the glass. The corroded layer on the surface of the glass is a silica gel. The corrosion process depends on several parameters such as temperature, pH, environment, glass composition and time.

Two models are available to describe the water behavior. Water enters the glass by an ionic exchange that involves the water protons and the alkaline or alkaline-earth ions of the glass:

$$\equiv\mathrm{Si{-}O^-M^+} + \mathrm{H_3O^+} \leftrightarrow \equiv\mathrm{Si{-}O{-}H} + \mathrm{M^+(aq)} + \mathrm{H_2O}$$

with M as alkali or alkali-earth element [27], and/or by diffusion according to the equation:

$$\equiv\mathrm{Si{-}O^-M^+} + \mathrm{H_2O} \leftrightarrow \equiv\mathrm{Si{-}O{-}H} + \mathrm{M^+(aq)} + \mathrm{OH^-}[28].$$

In both cases, the interaction between the glass and the water results in the loss of a cation ($M^+$) from the surface that will cause further migration of alkaline or alkaline-earth ions from the bulk to the surface. From a general point of view, the mobility of the ions in the glass depends on their role (glass-forming or network modifying) and is inversely proportional to their ionic radius. Corroded glass is generally depleted in K, Na, Ca and Mg and enriched in Si, Al, Ti and Fe compared to the pristine glass. However, the behavior of each element is difficult to predict and depends strongly on corrosion conditions. Whereas the alkaline earth elements (Ca, Mg) may remain in the altered glass layer, the alkaline elements are always heavily leached out. Phosphorus, manganese and trace elements will behave differently depending on the type of corrosion (atmospheric or underground). Some elements are retained in the corroded glass where they form mineral phases such as sulfates, carbonates or phosphates by precipitation with compounds present in the environment. In this study, strong depletion of soda indicates that highly corroded glass was sampled.

Six glass bead samples with the lowest soda concentrations according to the MURR measurements, ranging from 0.4 to 3.9% (Group C in Fig. 2) were selected. The corresponding soda concentrations as measured by the FM laboratory range from 11 to 22%. If it is assumed that the FM measurements correspond to the composition of pristine glass then, at least 78–96% of the soda initially present in the glass has disappeared in the corroded glass sampled by MURR. Other elements were variably affected by corrosion (Table 7) and are discussed below.

Potassium and magnesium are two elements depleted in the corroded glass samples, with two exceptions: samples PR768 and PR746 contain slightly more magnesia and more potash in their corroded layer compared to the pristine glass. Potassium from the soil can precipitate within the corroded glass as mineral phases such as syngenite ($K_2SO_4{\cdot}CaSO_4{\cdot}H_2O$), gorgeyte ($K_2SO_4{\cdot}5CaSO_4{\cdot}H_2O$) or polyhalite ($K_2SO_4{\cdot}2CaSO_4{\cdot}H_2O$) [29,30]. High concentrations of potassium in an archaeological soil may indicate the location of a fire, as this element is a major constituent of wood ash. In the corroded glass samples, lime is either depleted or the concentrations for this element in corroded and pristine glasses are extremely similar.

Glass-forming elements are supposed to be more stable than network-modifying elements: all of the corroded samples have higher alumina, iron and titanium concentrations than the pristine glass, with one exception. The corroded glass of sample PR719 is depleted in iron. Enrichment in glass-forming elements can be extremely important with, for example, a sixfold increase of the titanium concentration in the corrosion layer of sample PR781 or a threefold increase of the aluminum concentration in sample PR719.

Sample PR796 contains significantly higher phosphorus concentrations in the corroded glass compared to the pristine glass while we observe the opposite phenomenon for the other corroded samples. This is maybe due to the formation of hydroxyapatite ($Ca_5(PO_4)_3(OH)$), resulting from phosphorus available in the burial environment and generally associated with the former presence of organic debris such as excrement and plant tissue or the presence of bone [31].

Sample PR781 initially contained 1.3% manganese oxide. More than 8% of the same oxide was measured in the corroded glass. Such high concentrations of manganese are not unusual in corroded glass and were recorded locally, along cracks [32]. Whether the manganese found in high concentration in these corroded glasses comes from the burial environment or has migrated from within the glass is not clear. Watkinson et al. [32] demonstrated the ability of manganese to accumulate into a glass by migrating from the outside environment to the inside of the glass through cracks in the glass, forming dark insoluble compounds.

Most of the trace elements have higher concentrations in the corroded layer compared to the pristine glass, with the exception of lithium and arsenic (Table 8). The asterisk in Table 8 indicates cases where only five out of the six samples have some elemental enrichment and 15 times out of 17, it is PR719 that is different. Evolution of some of the trace elements in PR719 seems to differ from that in the five other corroded samples. For uranium, we observe a depletion for the lower concentrations (<2 ppm) and an enrichment for the highest concentrations (>30 ppm).

Previously published studies usually report ancient glass samples with similar compositions buried in the same soil environment. The behavior of the samples as a consequence is quite similar (e.g., [33–35]). For example, Sterpenich and Libourel [36] show systematic depletion for alkaline elements (Rb, Cs) and barium and some enrichment for the other elements in potash glass samples. However, glass artifacts from a single site may present quite different states of preservation, from totally intact to corroded to the core ([37] and pers. observation) even when the glass objects initially had the same composition. The results of this study are different again. First, the initial compositions of the six highly corroded samples were initially different; indeed, as discussed later, they belong to three different glass groups. Secondly, the samples studied here reflect a wide range of burial conditions with soils likely enriched in manganese, potassium or phosphorus. Finally, other parameters, like pH and red-ox conditions, may have varied and induced different corrosion phenomena. This study demonstrates that the analysis of highly corroded glass sample produces data from which it is difficult to reconstruct the initial composition of the glass.

### *4.4. Interpretation of the results*

Glass compositions reflect the type and source of the raw ingredients used by ancient glassmakers and therefore reflect the provenance of the glass, even if relating compositions and glass sources is often very difficult. Previous glass studies focused on the Sub-Saharan regions of Africa during the Islamic era between c.800 and 1500 CE revealed the presence of two major glass types. The first of these is characterized by relatively high alumina concentrations (higher than 4%) due to the addition of granite sand (containing relatively high levels of impurities) to mineral soda [38,39]. This glass

**Table 8**
List of the trace elements measured with LA-ICP-MS for the six most highly corroded samples with a summary of their behavior in corroded glass. D stands for depletion, E stands for enrichment, an asterisk means that only five samples out of the six are enriched in the corroded layer, NT stands for no trend, i.e., where at least two samples behave differently from the others for that element.

| Li | Co | Ni | Cu | Zn | As | Rb | Sr | Y | Zr | Nb | Mo | Sn | Sb | Cs | Ba | La | Ce |
|---|---|---|---|---|---|---|---|---|---|---|---|---|---|---|---|---|---|
| D | E* | E* | NT | NT | D | NT | E | NT | E | E* | NT | NT | NT | NT | NT | E* | E* |

| Pr | Nd | Sm | Eu | Gd | Tb | Dy | Ho | Er | Tm | Yb | Lu | Hf | Pb | Th | U |
|---|---|---|---|---|---|---|---|---|---|---|---|---|---|---|---|
| E* | E* | NT | E* | E* | E* | E* | E* | E* | E* | E* | NT | E* | E* | E | NT |

type is often called soda alumina glass or m-Na–Al glass. Based on trace element concentrations, two subtypes have been identified for this glass. The first subtype comprises glass samples mostly from South India, Sri Lanka and Southeast Asia, which date from the 5th c. B.C. to the 10th c. A.D. This glass, rare in Africa, has average uranium concentrations around 20 ppm and relatively high barium concentrations, up to approximately 3500 ppm. It is labeled low uranium–high barium glass or lU–hBa glass. The second subtype is more common at sites in Sub-Saharan Africa and on the west coast of India and dates from the 8th to the 19th c. A.D. [16]. This glass most likely comes from India and generally corresponds with the “trade wind beads” known to historians [40,41]. Uranium concentrations in this m-Na–Al glass are higher than in the previous subtype and average approximately 100 ppm, while barium concentrations are significantly lower; this subtype is labeled high uranium–low barium glass or hU–lBa glass [16].

The second type of glass is characterized by the use of plant ash (vegetal soda) instead of mineral soda as a flux. The concentrations of trace elements in this glass are rather low but alumina concentrations can vary in a wide range from about 1 to 8%.

Strontium, zirconium, barium and uranium concentrations can be used to discriminate, employing principal component analysis, between the glass types, as well as the subtypes of m-Na–Al glass (Fig. 6). For comparative purposes, Fig. 6 also includes samples belonging to the lU–hBa and hU–lBa groups [16] and to the vegetal soda group (Dussubieux, unpublished data).

Only one sample (PR205) falls in the lU–hBa subtype according to both laboratories. This bead is from Sri Lanka, which is consistent with the fact that this subtype of glass is extremely rare in Africa and much more common in Sri Lanka and South India. The two laboratories agree that the same 24 samples belong to the hU–lBa subtype. Corrosion did not seem to affect the reliability of the group attribution for these two subtypes. Uranium is an element that is very helpful in discriminating between the glass types, particularly since corrosion did not mask the patterns in the uranium concentrations. Uranium concentrations are very low (around 1 ppm) in the plant-ash (vegetal soda) glass and much higher in the m-Na–Al glass. Moreover, for the lU–hBa and hU–lBa glasses, the variability of uranium concentrations due to the sampling of corroded glass is less important than the variability of uranium between the two subtypes of glass.

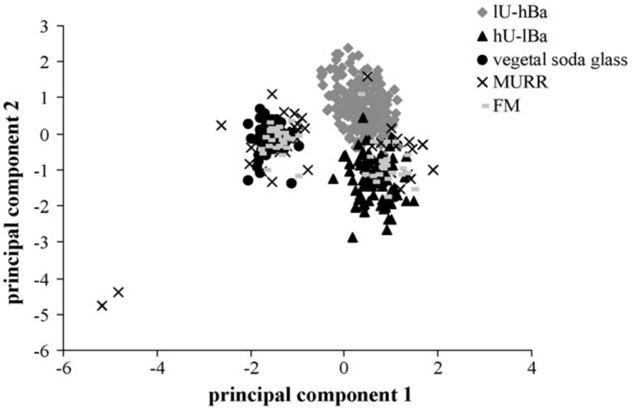

**Fig. 6.** Bi-plot of principal components 1 and 2 calculated from the concentrations of Sr, Ba, Zr and U for the 52 archaeological glass bead samples from this study and from samples of the different African glass types.

In Fig. 6, some samples form a tight group that overlaps with samples made of vegetal soda. Using the FM data for this glass type (since they are less affected by corrosion than the MURR data), two subtypes emerge according to the alumina concentrations: a “low” alumina glass (<4%) and a “high” alumina glass (>4%) (Fig. 7). Turning to the MURR data, four samples (PR719, PR781, PR793 and PR796) have especially high alumina concentrations; these measurements can be best explained by the fact that these beads were all extremely corroded. Apart from these four highly corroded beads, the MURR measurements shown in Fig. 7 also fall into two groups with a limit for the alumina concentrations at 4.5%, which is very close to the limit proposed according to the FM measurements and well within the 20% range defined for the relative deviations between the concentrations measured by the FM and MURR laboratories. The low alumina, vegetal soda glass is similar to the Islamic glass that was dominant across much of the Islamic world beginning about the 8th to 10th centuries A.D. [42,43]. The high alumina, vegetal soda glass has been identified in the form of beads at many sites in Sub-Saharan Africa, particularly in southern Africa and Madagascar; a South or Southeast Asian origins has been tentatively proposed [11,17,18], though more research is needed on

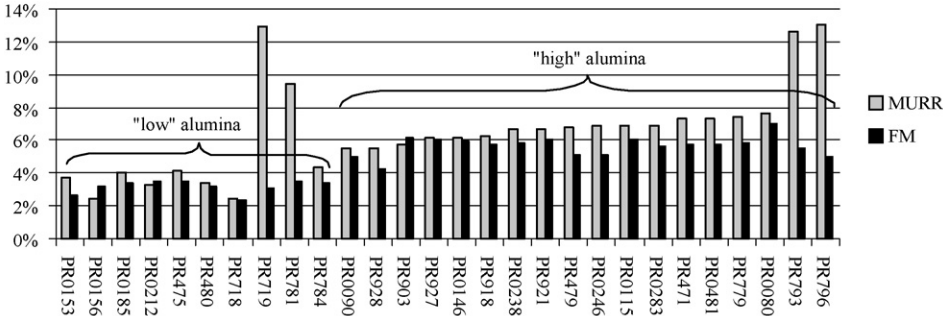

**Fig. 7.** Alumina concentrations as determined by MURR and FM of the 28 vegetal soda glass samples identified by principal component analysis.

this glass, particularly to determine the geological character of the sand used in its manufacture.

There are two samples, both based on MURR measurements, shown in Fig. 6 that fall well outside the parameters of the types and subtypes discussed above. PR781 and 793 are two extremely corroded beads that cannot be attributed to any glass type.

## 5. Conclusion

The results of the analyses of 52 glass samples in two different laboratories using LA-ICP-MS show good agreement despite some discrepancies. These discrepancies are due to different factors. First, different instrumentations and protocols were used by the two laboratories, and more especially different ablation modes. Second, the heterogeneous distribution of some elements involved in the coloring and/or opacifying process of the glass has an impact on the results. While measurements of these elements may be very useful for understanding the glass technologies mastered by the ancient glassmakers, they are, with few exceptions (e.g., cobalt), of little interest when determining the provenance of the glass. Finally, corrosion is also a major factor that influenced the compositions measured using LA-ICP-MS. The raster method, even when a pre-ablation is performed to clean the surface to be sampled, was found to be more sensitive to corrosion as it allowed the sampling of material closer to the surface than was the case when the single point mode of sampling with a pre-ablation time of approximately 20 s was employed. In only two cases involving MURR results, did corrosion prevent an attribution of the glass to any glass type. In a further four samples identified as belonging to the plant-ash type corrosion induced a high increase in their alumina concentrations (as measured at MURR) and therefore jeopardized a more precise identification of the glass type to which they belong. Overall, LA-ICP-MS is a reliable and minimally destructive method for determining the composition of ancient glass, including minor, major and trace elements. It can also be employed with confidence on glass samples exhibiting surface corrosion provided the single point sampling method is used.

## Acknowledgments

We would like to thank James Lankton for first drawing our attention to the importance of comparing the FM and MURR results. Rachel Popelka-Filcoff carried out the LA-ICP-MS analysis at MURR. Marilee Wood's expertise in the identification and history of glass beads has been invaluable in all phases of our research.

The LA-ICP-MS laboratory at the Field Museum of Natural History was built with funds from the National Science Foundation (BCS-0320903), an anonymous donation, and the Anthropology Alliance. The analysis of the PR bead samples and the larger project from which it stems was funded by the National Science Foundation (BCS-0209681).

## References

[1] B. Gratuze, A. Giovagnoli, J.-N. Barrandon, P. Telouk, J.-L. Imbert, Apport de la méthode ICP-MS couplée à l'ablation laser pour la caractérisation des archéomatériaux, Rev. Archéom. 17 (1993) 89–104.
[2] P. Telouk, Développement de la spectrométrie ICP-MS dans le domaine de l'archéologie et de la géologie—utilisation de l'ablation laser, Unpublished Ph.D. Thesis, Université Claude Bernard, Lyon I, France, 1993.
[3] M. Motelica-Heino, P. Le Coustumer, O.F.X. Donard, Micro- and macro-scale investigation of fractionation and matrix effects in LA-ICP-MS at 1064 nm and 266 nm on glassy materials, J. Anal. At. Spectrom. 16 (2001) 542–550.
[4] A.J.C. Mank, P.R.D. Mason, A critical assessment of laser ablation ICP-MS as an analytical tool for depth analysis in silica-based glass samples, J. Anal. At. Spectrom. 14 (1999) 1143–1153.
[5] K. Smith, T. Trejos, R.J. Watling, J. Almirall, A guide for the quantitative elemental analysis of glass using laser ablation inductively coupled plasma mass spectrometry, At. Spectr. 27 (7) (2006) 69–75.
[6] M. Blet, L'apport de l'ablation laser couplée à l'ICP-MS, à la caractérisation des archéomatériaux siliceux, Unpublished Ph.D. Thesis, Université d'Orléans, France, 1999.
[7] B. Gratuze, M. Blet-Lemarquand, J.-N. Barrandon, Mass spectrometry with laser sampling: a new tool to characterize archaeological materials, J. Radioanal. Nucl. Chem. 247 (3) (2001) 645–656.
[8] B. Gratuze, Obsidian characterization by laser ablation ICP-MS and its application to prehistoric trade in the Mediterranean and the Near East: sources and distribution of obsidian within the Aegean and Anatolia, J. Archaeol. Sci. 26 (8) (1999) 869–881.
[9] S.J. Saitowitz, Glass beads as indicators of contact and trade in Southern Africa ca AD 900–AD 1250, Unpublished Ph.D. Thesis, University of Cape Town, South Africa, 1996.
[10] S.J. Saitowitz, D.L. Reid, N.J. Van der Merwe, Glass bead trade from Islamic Egypt to South Africa c. AD 900-1250, S. Afr. J. Sci. 92 (1996) 101–104.
[11] P. Robertshaw, B. Rasoarifetra, M. Wood, E. Melchiorre, R.S. Popelka-Filcoff, M.D. Glascock, Chemical analysis of glass beads from Madagascar, J. Afr. Archaeol. 4 (2006) 91–109.
[12] I. De Raedt, K. Janssens, J. Veeckman, L. Vincze, B. Vekemans, T.E. Jeffries, Trace analysis for distinguishing between Venetian and façon-de-Venise glass vessels of the 16th and 17th century, J. Anal. At. Spectrom. 16 (2001) 1012–1017.
[13] Ž. Šmit, K. Janssens, E. Bulska, B. Wagner, M. Kos, I. Lazar, Trace element fingerprinting of façon-de-Venise glass, Nucl. Instrum. Methods Phys. Res. B: Beam Interact. Mater. At. 239 (2005) 94–99.
[14] L. Dussubieux, B. Gratuze, Origine et diffusion du verre dans le monde indien et en Asie du Sud-est: l'importance du dosage des éléments-traces, Rev. Archéom. 27 (2003) 67–73.
[15] A. Shortland, N. Rogers, K. Eremin, Trace element discriminants between Egyptian and Mesopotamian late bronze age glasses, J. Archaeol. Sci. 34 (5) (2007) 781–789.
[16] L. Dussubieux, C.M. Kusimba, V. Gogte, S.B. Kusimba, B. Gratuze, R. Oka, The trading of ancient glass beads: new analytical data from South Asian and East African soda-alumina glass beads, Archaeometry 50 (5) (2008) 797–821.
[17] R.S. Popelka, M.D. Glascock, P. Robertshaw, M. Wood, Laser ablation ICP-MS of African glass trade beads, in: R.J. Speakman, H. Neff (Eds.), Laser Ablation ICP-MS in Archaeological Research, University of New Mexico Press, Albuquerque, NM, 2005, pp. 84–93.
[18] P. Robertshaw, M.D. Glascock, M. Wood, R.S. Popelka, Chemical analysis of ancient African glass beads: a very preliminary report, J. Afr. Archaeol. 1 (2003) 139–146.
[19] H. Neff, Analysis of Mesoamerican plumbate pottery surfaces by laser ablation-inductively coupled plasma-mass spectrometry (LA-ICP-MS), J. Archaeol. Sci. 30 (1) (2003) 21–35.
[20] R.J. Speakman, H. Neff, The application of laser ablation—ICP-MS to the study of archaeological materials—an introduction, in: R.J. Speakman, H. Neff (Eds.), Laser Ablation ICP-MS in Archaeological Research, University of New Mexico Press, Albuquerque, NM, 2005, pp. 1–14.
[21] N.J.G. Pearce, W.T. Perkins, J.A. Westgate, M.T. Gorton, S.E. Jackson, C.R. Neal, S.P. Chenery, A compilation of new and published major and trace element data for NIST SRM 610 and SRM 612 glass reference materials, Geostandard Newslett. XXI (1997) 114–115.
[22] R.H. Brill, Chemical analyses of early glasses, vol. 2, The Corning Museum of Glass, New York, 1999.
[23] J.J. González, A. Fernández, X. Mao, R.E. Russo, Scanning vs. single spot laser ablation ($\lambda = 213$ nm) inductively coupled plasma mass spectrometry, Spectrochim. Acta B: At. Spectrosc. 59 (3) (2004) 369–374.
[24] H.P. Rooksby, A yellow cubic lead tin oxide opacifier in ancient glasses, Phys. Chem. Glasses 5 (1) (1964) 20–25.
[25] B. Gratuze, I. Soulier, M. Blet, L. Vallauri, De l'origine du cobalt: du verre à la céramique, Rev. Archéom. 20 (1996) 77–94.
[26] B. Gratuze, I. Soulier, J.-N. Barrandon, D. Foy, De l'origine du cobalt dans les verres, Rev. Archéom. 16 (1992) 97–108.
[27] R.H. Doremus, Interdiffusion of hydrogen and alkali ions in a glass surface, J. Non-Cryst. Solids 19 (1975) 137–144.
[28] B.M.J. Smets, T.P.A. Lommen, The role of molecular water in the leaching of glass, Phys. Chem. Glasses 24 (1983) 35–36.
[29] J. Henderson, S.E. Warren, X-ray fluorescence analyses of iron age glass: beads from Meare and Glastonbury lake villages, Archaeometry 23 (1) (1981) 83–94.
[30] W. Geilmann, H.T. Berthold, G. Tölg, Beiträge zur Kenntnis alter Gläser V. Die Verwitterungsprodukte auf Fensterschieben, Glastechniche Beritche 33 (1960) 213–219.
[31] I.C. Freestone, N.D. Meeks, A.P. Middleton, Retention of phosphate in buried ceramics: an electron microbeam approach, Archaeometry 27 (2) (1985) 161–177.
[32] D. Watkinson, L. Weber, K. Anheuser, Staining of archaeological glass from manganese-rich environments, Archaeometry 47 (1) (2005) 69–82.
[33] M. Garcia-Vallès, D. Gimeno-Torrente, S. Martínez-Manent, J.-L. Fernández-Turiel, Medieval stained glass in a Mediterranean climate: typology, weathering and glass decay, and associated biomineralization processes and products, Am. Miner. 88 (2003) 1996–2006.
[34] A. Silvestri, G. Molin, G. Salviulo, Archaeological glass alteration products in marine and land-based environments: morphological, chemical and microtextural characterization, J. Non-Cryst. Solids 351 (2003) 1338–1349.

[35] R. Prochazka, Natural corrosion of the uranium-colored historical glasses, J. Non-Cryst. Solids 353 (2007) 2052–2056.
[36] J. Sterpenich, G. Libourel, Using stained glass windows to understand the durability of toxic waste matrices, Chem. Geol. 174 (2001) 181–193.
[37] I. Glover, Differential decay of buried iron age Thai glass in a uniform environment, in: M.M.</In> Wright (Ed.), Ethnographic Beadwork, Aspects of Manufacture, Use and Conservation, Archetype Publications, Ltd., London, 2001, pp. 15–26.
[38] R.H. Brill, Chemical analyses of some early Indian glasses, in: H.C. Bhardwaj (Ed.), Archaeometry of Glass, Proceedings of the Archaeometry Session of the XIV International Congress on Glass 1986, New Delhi, India, Section 1, India Ceramic Society, Calcutta, 1987, pp. 1–25.
[39] J.W. Lankton, L. Dussubieux, Early glass in Asian maritime trade: a review and an interpretation of compositional analyses, J. Glass Stud. 48 (2006) 121–144.
[40] W.G.N. Van der Sleen, Trade wind beads, Man 56 (1956) 27–29.
[41] P. Francis Jr., Asia's Maritime Bead Trade 300 B.C. to the Present, University of Hawaii Press, Honolulu, 2002.
[42] R.H. Brill, Some thoughts on the chemistry and technology of Islamic glass, in: S. Carboni, D. Whitehouse (Eds.), Glass of the Sultans, Yale University Press, New Haven–London, 2001, pp. 25–45.
[43] J. Henderson, S.D. McLoughlin, D.S. McPhail, Radical changes in Islamic glass technology: evidence for conservatism and experimentation with new glass recipes from early and middle Islamic Raqqa, Syria, Archaeometry 46 (3) (2004) 439–468.